Mechanical Properties and Failure Behavior of Hexagonal Boron Nitride–Graphene van der Waals Heterostructures through Molecular Dynamics Simulation

S. Rabet*, H. R. Ovesy*, A. Ramazani**

* Aerospace Engineering Department, Amirkabir University of Technology, Hafez Ave, Tehran, Iran
** Department of Mechanical Engineering, Massachusetts Institute of Technology, Cambridge, MA 02139, USA

ARTICLE HISTORY
Compiled April 7, 2019

ABSTRACT
Molecular dynamics(MD) simulations are carried out to characterize the mechanical properties and failure behavior of van der Waals heterostructures composed of graphene and hexagonal boron nitride(hBN) single layer sheets. The graphene–hBN and hBN–graphene–hBN heterostructures simulations are carried out under tensile and shear deformation. Accordingly, stress versus strain curves of each system are plotted and various properties of heterostructures, namely elastic modulus and shear modulus as well as failure stress and failure strain, are evaluated and compared with one another as well as with the pristine graphene and hBN sheets. Subsequently, the failure mechanism/characterization of each sheet in the heterostructures is described. Alternatively, the elastic and shear modulus of each heterostructure are computed by means of rule of mixture(ROM) which are in good agreement with results that are obtained from MD simulations.

Keywords: Mechanical properties; graphene; hexagonal boron nitride; van der Waals heterostructures; molecular dynamics

1. Introduction

In the last couple of years, researches on two-dimensional atomic crystals have attracted great attention as a result of their extraordinary electrical, mechanical and optical properties. Recently, another outstanding topic that has emerged is van der Waals (vdW) heterostructures. These kinds of materials are made by assembling different 2D materials on top of each other [1]. By means of this approach, researchers can achieve materials with arbitrary properties. A kind of vdW heterostructures made of graphene and hexagonal boron nitride achieve a great deal of attention among 2D heterostructures in that they possess unique optical and electrical properties. The outstanding mechanical properties of graphene that made of carbon atoms in honeycomb lattice structure are reported in previous articles [2, 3]. Structural lattice of hexagonal boron nitride has a similar arrangement with boron and nitrogen atoms and both

CONTACT A. Ramazani. Email: ramazani@mit.edu

of them have strong sp^2 bonds [4]. There is a slight mismatch between the lattice constants of hBN and graphene sheets (about 1.8%), which has caused the moir pattern to form [5, 6]. This pattern has led to some fascinating characteristics in these vdW heterostructures [7, 8]. HBN is a high-quality substrate for graphene layer which could lead to the development of high-performance graphene devices [6]. Moreover, encapsulating a graphene sheet between hBN layers, i.e. hBN/graphene/hBN, could keep graphene and prevent its properties from declining under ambient conditions [9]. Moreover, this heterostructure could be utilized in field effect transistors to greatly improve radio-frequency applications [10]. Thus, the investigation of heterostructures mechanical properties as well as studying their chemical and electrical characteristics have a crucial role for proper use of these novel kinds of materials.

In this research the properties of hBN/graphene, i.e.(BG), and hBN/graphene/hBN, i.e.(BGB), vdW heterostructures under shear and tensile loads have been investigated. Molecular dynamics(MD) approach is used to study these heterostructures and the results are compared with single layer graphene and hBN sheets. MD simulations of heterostructures and single layers are performed by Large-scale Atomic/Molecular Massively Parallel Simulator (LAMMPS) [11] and visualization is carried out with OVITO [12] software.

2. Simulation Models and Method

In atomistic simulations, the selection of proper force-field which simulates the characteristics of a desired system accurately and completely is of paramount importance. The adaptive intermolecular reactive empirical bond order (AIREBO) potential [13] is a force-field which is widely employed [14, 15] to describe interactions between carbon atoms in graphene sheets, and it is utilized to model the formation and breakage of links between carbon atoms in this study. AIREBO potential consists of three covalent, torsional and Lennard-Jones terms and the equation is

$$E^{AIREBO} = \frac{1}{2}\sum_{i}\sum_{i\neq j}[E_{ij}^{REBO} + \sum_{k\neq i.j}\sum_{l\neq i.j.k} E_{ijkl}^{TORSION} + E_{ij}^{LJ}] \tag{1}$$

Where E^{AIREBO} is the total energy of the system; E_{ij}^{REBO} is the REBO term which describes potential between covalently bonded atoms; $E_{ijkl}^{TORSION}$ is the torsional part of the potential which depends on dihedral angle and E_{ij}^{LJ} is the Lennard-jones term which represents the intermolecular van der waals interactions and also, i, j, k and l are the indices for atoms. The $2\dot{A}$ cut-off distance is applied in AIREBO potential in order to avoid nonphysical strain-hardening effect [16]. In this research, Tersoff [17] potential is used for modeling interactions between boron and nitrogen atoms in hBN. The cut-off distance for this force-field also should be modified to eliminate the overestimation of stress for breakage of the sheet. Accordingly, the minimum cut-off distance is considered equal to the maximum one. Moreover, interactions between graphene sheet and hBN sheet are described by non-bonded van der Waals force which is modeled by means of Lennard-Jones 12-6 potential as

$$E_{(r)}^{LJ} = 4\epsilon[(\frac{\sigma}{r})^{12} - (\frac{\sigma}{r})^{6}] \tag{2}$$

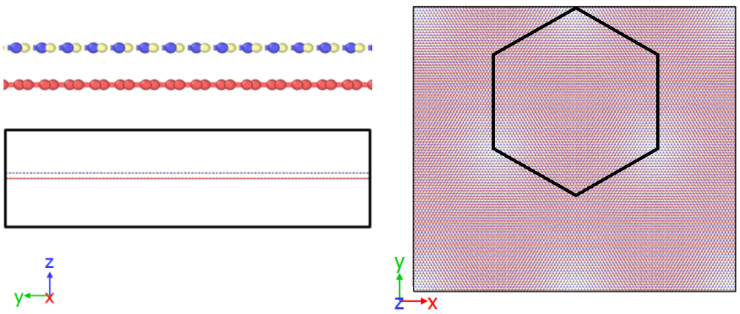

Figure 1.. Structure of graphene-boron nitride heterostructure(BG).

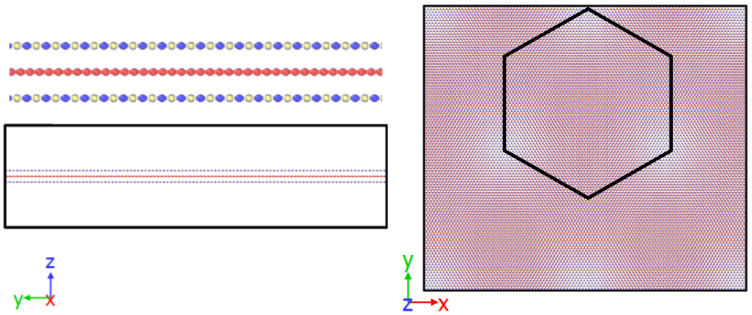

Figure 2.. Structure of boron nitride-graphene- boron nitride heterostructure(BGB).

where ε and σ are energy and distance parameters that are evaluated with Lorentz combining rules [11] for interaction between atoms in graphene and hBN sheets. Thus, Lennard-Jones parameters for van der Waals interactions between B(Boron), C(Carbon) and N(Nitrogen) atoms are $\epsilon_{CB} = 3.411\dot{A}$, $\epsilon_{CN} = 3.667\dot{A}$, $\sigma_{CB} = 3.311meV$ and $\sigma_{CN} = 4.068meV$ and the distance between each layer of graphene sheet with a layer of boron nitride sheet is considered as $3.4\dot{A}$ so that the heterostructure has minimum vdW energy [8].

Lattice constant for graphene sheets is $1.42\dot{A}$ and for hBN sheets is $1.446\dot{A}$ and due to this difference hBN and graphene single layers cannot completely match to each other. Therefore, a graphene sheet and a hBN sheet should be integrated in a way that they have smallest internal strain energy for vdW heterostructures [18] and the edges of both hBN and graphene sheets match with the periodic boundary condition of the system. For this purpose, the graphene and the hBN which are studied in this research have dimension about $224\dot{A}$ in zigzag direction and $254\dot{A}$ in armchair direction. Thus, the length alteration of $0.01\dot{A}$ and $0.08\dot{A}$ in zigzag and armchair direction is provided respectively. The obtained BG vdW heterostructure and BGB heterostructure are shown in Figures. 1 and 2 respectively, and in these figure moir pattern in hexagonal shape and specific periodicity could be seen in BG and BGB layer.

At the beginning of each simulation, a system is optimized and then equilibrated with NPT(isothermal-isobaric) ensemble under 300K temperature and zero pressure. All of the simulations are performed by time step of $1fs$ with periodic boundary condition(PBC). After equilibration, the tensile or shear load is applied with strain rate of $0.001(Ps)^{-1}$ by deformation control method which is previously utilized for these kinds of modeling [19, 20].

2.1. Tensile Test

In this section, the tensile test of graphene single layer and hBN sheets and also their vdW heterostructures(i.e. BG and BGB) are investigated. The thickness of a single layer hBN and a graphene sheet is considered as $t = 3.4\dot{A}$, which is equal to the sheets distance from each other in z direction due to the vdW interaction [8]. Stress-strain curve of each sheet or heterostructure is extracted by means of NPT ensemble with 300K temperature while pressure on perpendicular directions to loading direction is set to be zero in order to make the model stress free in other directions that are not loaded. The stress tensor in molecular simulations, consisting of a virial term and a kinetic term, describes the effect of temperature, pairs, bonds, angels and etc. [21]. The global stress tensor for a specific number of particles is computed by the formula

$$P = \frac{1}{V}(\sum_{i=1}^{N} m_i v_i \otimes v_i + W(r^N)) \tag{3}$$

Where P is the global stress tensor and V is the volume of N particles; m_i and v_i are the velocity and mass of atom i, respectively. The global virial term is shown with W which can be obtained by the expression

$$W(r^N) = \sum_{i=1}^{N} r_i \cdot F_i \tag{4}$$

Where r_i is the position of i^{th} atom. F_i is the total force on atom i which is resulted from interactions between the atom i and other atoms.

The total volume of each single layer sheet is calculated with the $3.4\dot{A}$ thickness. Each system is loaded in both armchair and zigzag directions which are defined with direction of load according to sheets edges(Figure. 3) and their stress-strain curves are plotted. When fracture occurs in sheets or heterostructures, a drastic decrease is observed in stress-strain curve.
The Young's modulus (E) can be extracted from the initial linear slope of the stress-

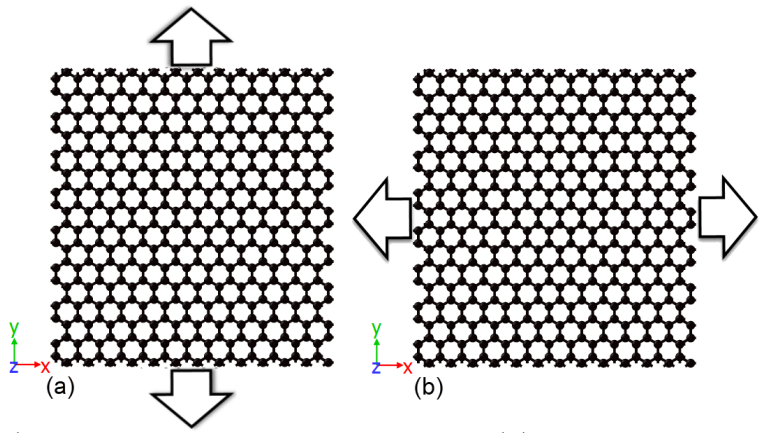

Figure 3.. (a)Tensile test in armchair direction and(b) Tensile test in zigzag direction.

strain curve. The ultimate tensile strength(σ_{ult}) and failure strain(ϵ_f) can also be ob-

tained from the peak point of the corresponding curve where one of the sheets(graphene or hBN) is failed.

2.2. Shear Test

After minimization and equilibration of a system the shear load is applied by deformation control method. The deformation is applied by shear strain rate of $0.001(Ps)^{-1}$ in armchair or zigzag directions as shown in Figure. 4. The system temperature is controlled in 300K with Nose-Hoover thermostat. For a specific strain, the corresponding shear stress is computed through the application of Equation (3). The shear modulus(G) of graphene, hBN sheet and heterostructures is computed by evaluating the initial linear slope of the shear stress-strain curve. The shear strength (σ_{sf}) and the shear fracture strain (ϵ_{sf}) correspond to the point where the first sudden decrease in the curve is experienced.

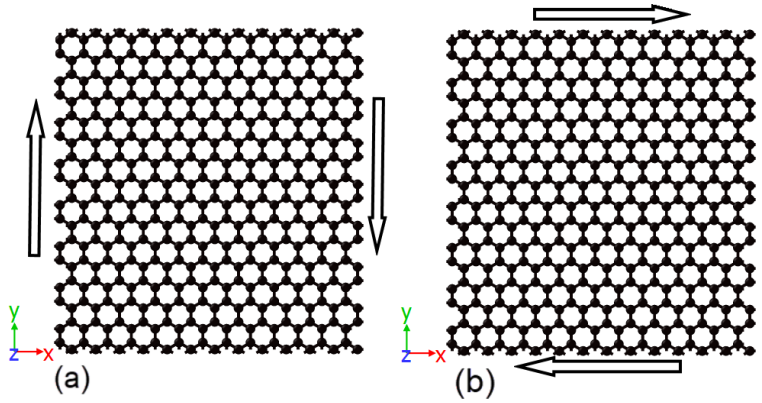

Figure 4.. (a)Shear deformation in armchair direction and (b)Shear deformation in zigzag direction.

3. Results and Discussion

At the beginning of the simulation, the structure of each vdW heterostructure in the LAMMPS is optimized(i.e. the enrgy of the system is minimized) in order to relax the structure. After optimization, the moire pattern periodicity could be seen for the out of plane deformation(δ) of the heterostructures. The wavelength of moire pattern(L) is measured about $13\dot{A}$ for hBN-graphene heterostructure which is in a good agreement with the previous measurement [7]. This pattern is formed in order to provide a minimum energy in the heterostructure with minimizing the mismatch between layers. Therefore, some regions of the sheet are stretched and some other parts are compressed. In Figure. 5 the nondimentional out of plane deformation(δ/t) of graphene and hBN sheets in the BG and BGB heterostructures is shown. The moir pattern can be clearly seen in these pictures. At this stage, the structure has become ready for the equilibration action to be carried out.

Subsequent to the appropriate equilibration, the tensile simulation of graphene and hBN single layer sheets as well as their heterostructures are carried out in both armchair and zigzag directions. Figure. 6 represents the stress versus strain curve for a

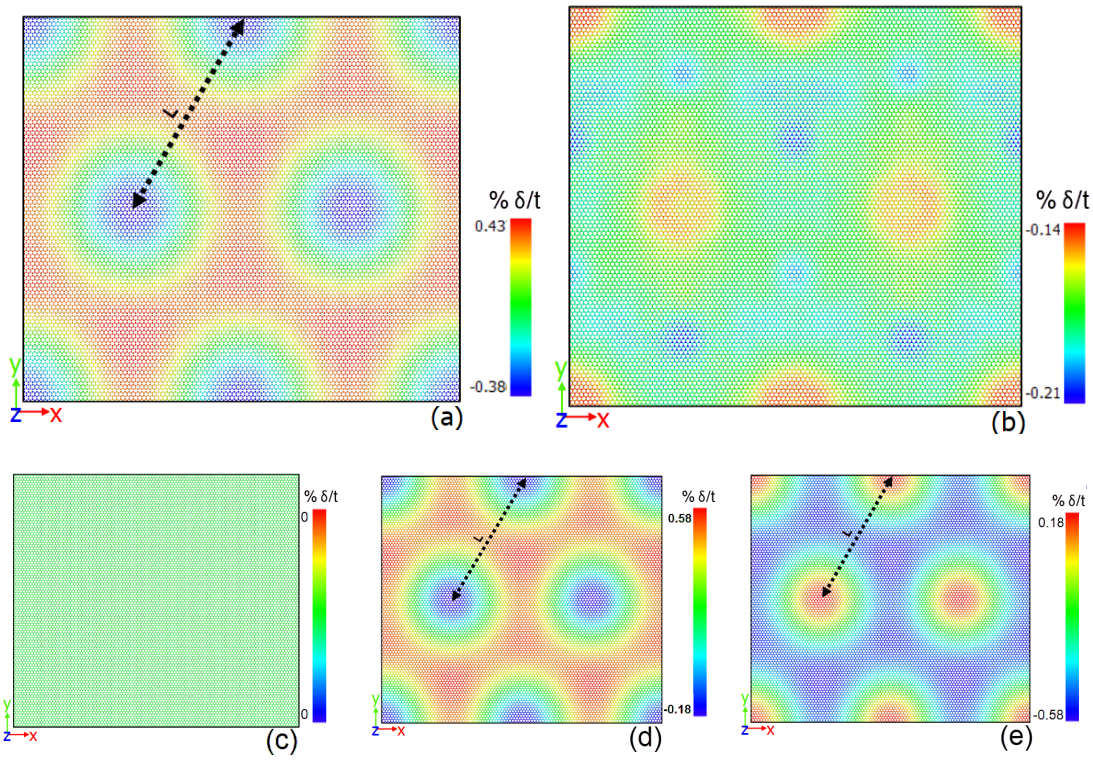

Figure 5.. out of plane deformation of (a) graphene, (b) hBN sheet in BG heterostructure and (c) graphene sheet, (d) one of the hBN sheet and (e) another hBN sheet in BGB heterostructure.

graphene and a hexagonal boron nitride single layer sheet. In the same figure, BG and BGB heterostructures under tensile load in both armchair and zigzag direction are also presented. The failure of both BG and BGB heterostructures in both armchair and zigzag directions begins with graphene rupture but hBN sheets endure the load(for 1-3Ps) until they collapse. The fractured graphene and hBN sheet in BG construction are shown in Figure. 7. The similar fractured individual sheets in the BGB construction are shown in Figure. 8.

As presented in Figures. 7 and 8 , the crack propagation in graphene single layer sheets occurs along zigzag direction while the loading is in armchair direction. However, the crack spreads in diagonal directions in the case of zigzag loading. This happens due to graphenes tendency to fail along the zigzag direction since the armchair edge has a higher edge energy level [14]. The hBN sheets failure pattern is also similar to the pattern that has been reported in ref [22], which applies Seviks modification on Tersoff potential. Similar to that reported in ref [22] with respect to hBN, due to its ductile fracture, some chains are formed in failure region.

The young's modulus and σ_{ult} also ϵ_f , that correspond to graphene and hBN single layer, are shown in Tables 1. and 2. The results are in good agreement with previous researches [14, 22, 23, 24]. The discrepancy between the results of this research and other references is due to the difference between size of the sheet and the temperature of the system which is resulted to more ripples existence with larger amplitude. It is expected that the youngs modulus and fracture strength and strain of graphene and hBN sheet decrease with the increase in temperature [20]. Moreover, it should be

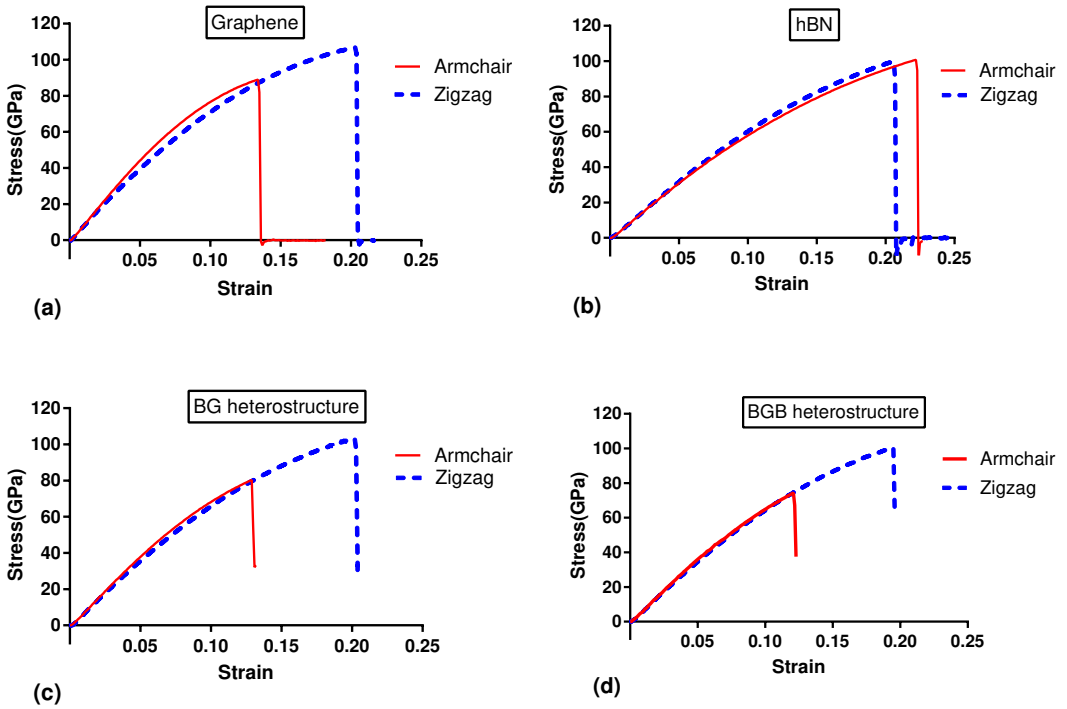

Figure 6.. stress-strain curve for (a) Graphene sheet, (b) hBN sheet, (c) BG heterostructure and (d) BGB heterostructure under tensile load.

Table 1.. Elastic modulus, ultimate strength and failure strain of a graphene sheet.

	E(Gpa)	E(GPa) refrences	σ_{ult}(GPA)	σ_{ult}(GPa) refrences	ϵ_f
Armchair	911	1112 [14], 1000100 [23]	88.7	88.5 [14], 13010[23]	0.138
Zigzag	808	897 [14]	106.9	105.5 [14]	0.203

Table 2.. Elastic modulus and ultimate strength and failure strain of a hBN sheet.

	E(Gpa)	E(GPa) refrences	σ_{ult}(GPA)	σ_{ult}(GPa) refrences	ϵ_f
Armchair	641	630 [24], 723 [22]	100.5	104[24], 94.1 [22]	0.221
Zigzag	655	733 [22]	99.9	100.3 [22]	0.206

considered that most of the pervious tensile tests are implemented on square shape sheets but in this article the layers are rectangular in order to be integrated properly.

Mechanical properties of BG and BGB heterostructures have been obtained from stress-strain curves of Figure. 6 and they are represented in Table 3. It is demonstrated that elastic modulus of BG and BGB has a value between elastic modulus of hBN and graphene single layer sheets while ϵ_f for both heterostructures is lower than fracture strain of each single layer sheet individually. This might have occurred due to the size

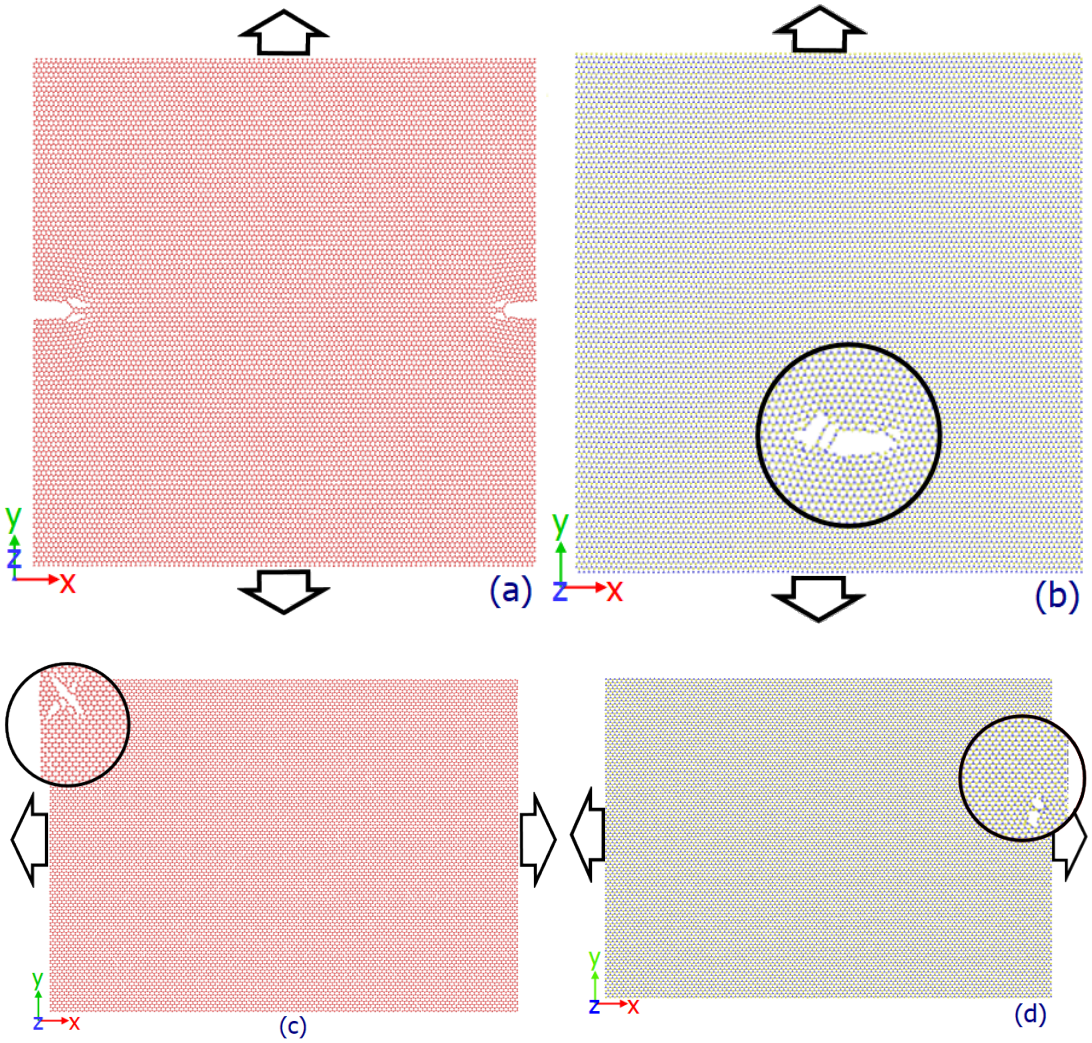

Figure 7.. Failure of single layers in BG heterostructure (a) graphene and (b) hBN in armchair tensile test, (c) graphene and (d) hBN in zigzag tensile test.

Table 3.. Elastic modulus and ultimate strength and failure strain of BG and BGB heterostructure

	BG heterostructure			BGB heterostructure		
Direction	E(Gpa)	σ_{ult}(GPa)	ϵ_f	E(Gpa)	σ_{ult}(GPa)	ϵ_f
Armchair	787	80.3	0.129	741	74.2	0.120
Zigzag	740	103.6	0.202	714	100.7	0.194

difference between graphene and hBN sheets which has led to intrinsic strain energy due to initial strain in layers. Thus, the graphene layer fails first in BG and BGB heterostructures at lower strain than that for pristine graphene.

In another attemp, the shear test modeling is performed on single layer sheets and heterostructures as discussed earlier. The shear stress-strain curve of graphene and hBN single layer and also BG and BGB are depicted in Figure. 9. The failure of the graphene sheet in BG and BGB heterostructures has occurred first. after some time-

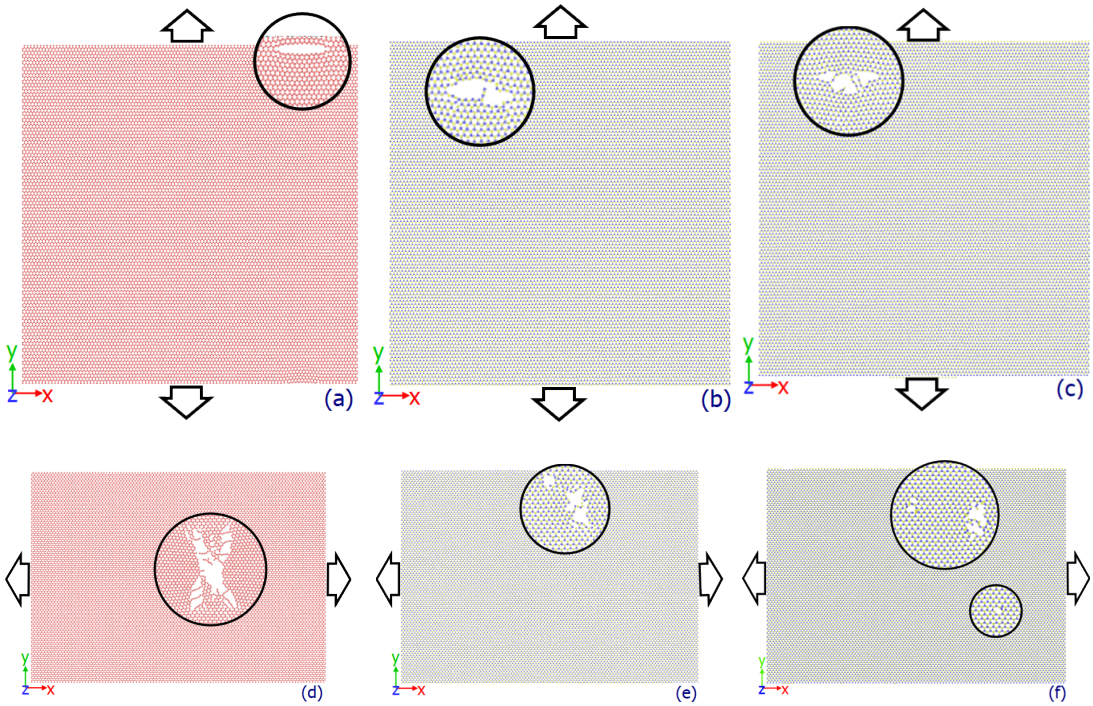

Figure 8.. Failure of each layers in BGB heterostructure (a) graphene, (b) one of the hBN sheets and (c) another hBN sheets in armchair direction and also (d) graphene, (e) one of the hBN layers and (f) another hBN sheets in zigzag direction

steps(20-80Ps), which take longer than those of the tensile test, the hBN sheets in both of the heterostructures fracture. It occurs as a result of the hBN sheet having a larger shear fracture strain and consequently withstanding higher shear strain in BG and BGB heterostructures. Two intense decreases in stress are observed in the shear stress-strain curve of BG and BGB heterostructure. The first one refers to the failure of graphene sheet and the second one corresponds to hBN sheet(s) failure. The second failure point varies between different heterostructures since after the fracture of the graphene, systems do not have stable situation as the atoms of the ruptured sheets move randomly in the simulation box. The shear modulus(G) and shear fracture stress (σ_{sf}) and shear fracture strain(ϵ_{sf}) of each sheet as well as those of heterostructures are given in Table 4. The results are validated with some previous researches wherever available. It is shown that G is almost the same in armchair and zigzag direction but shear fracture stress has a lower value in armchair direction. In addition, both shear modulus(G) and shear fracture stress(σ_{sf}) have lower values in BG and BGB heterostructures than pristine single layer sheets of graphene and hBN.

The expected elastic or shear modulus of BG and BGB heterostructures(M_{hetero}) can be computed by using the graphene and hBN elastic modulus in Tables 1. and 2. through the application of rule of mixture(ROM):

$$M_{hetero} = M_G f_G + M_{BN} f_{BN} \tag{5}$$

Where M_G and M_{BN} are elastic or shear modulus of a graphene single layer and hBN sheet, respectively; f_G and f_{BN} are volume fraction of these single layer sheet in the corresponding heterostructures, i.e., f_G is equal to $\frac{1}{2}$ in BG and $\frac{1}{3}$ in BGB. The

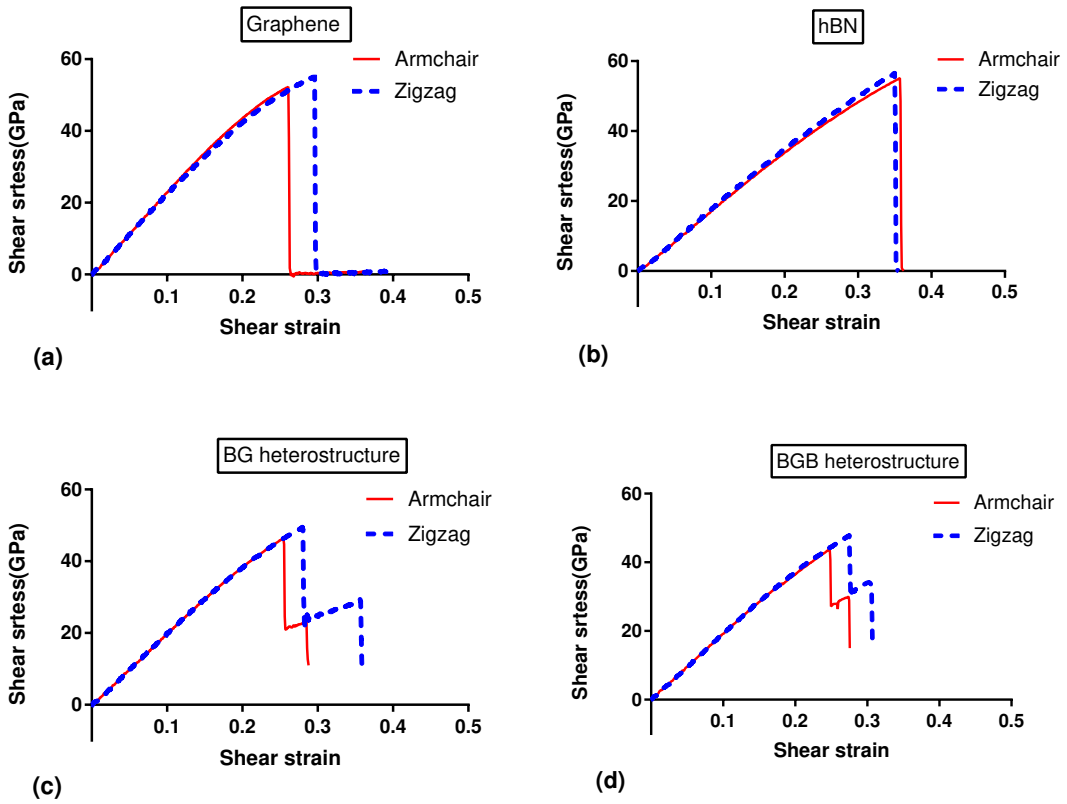

Figure 9.. Shear stress-strain curve of (a)graphene sheet, (b)hBN sheet, (c)BG heterostructure and (d)BGB heterostructure.

Table 4.. Mechanical properties of single layer sheets and heterostructures under shear deformation

sheet	Direction	G(Gpa)	G(Gpa) references	σ_{sf}(GPa)	ϵ_{sf}
Graphene	Armchair	228	228 [25], 280 [26]	52	0.26
	Zigzag	226	213 [25], 280 [26]	55	0.30
hBN	Armchair	166	190 [27]	55	0.36
	Zigzag	167	190[27]	56.5	0.35
BG	Armchair	198	-	46.5	0.25
	Zigzag	197	-	50	0.28
BGB	Armchair	192	-	44	0.25
	Zigzag	190	-	48	0.28

elastic modulus and shear modulus of BG and BGB heterostructures, which have been obtained from molecular dynamics simulation, and those computed by ROM method are given in Table 5.

A very good agreement can be seen among the MD and ROM results. It is noted that the MD elastic and shear modulus of both heterostructures either in armchair or zigzag directions are slightly higher than those of ROM approach. This might have occurred due to the existence of von der Waals interaction between graphene and hBN sheets

Table 5.. Elastic modulus of BG and BGB heterostructures by MD and ROM method.

	BG heterostructure		BGB heterostructure		BG heterostructure		BGB heterostructure	
Direction	E_{ROM} (GPa)	E_{MD} (GPa)	E_{ROM} (GPa)	E_{MD} (GPa)	G_{ROM} (GPa)	G_{MD} (GPa)	G_{ROM} (GPa)	G_{MD} (GPa)
Armchair	776	787	731	741	197	198	187	192
Zigzag	732	740	706	714	196.5	197	187	190

in MD simulation. Similar outcome has also been reported in some previous studies related to other heterostructers [18, 28].

4. Conclusions

The mechanical properties of BG and BGB heterostructures which consist of graphene and hBN single layer sheets have been studied in this research. The stress-strain curve of each single layer sheet and heterostructure has been plotted under shear and tensile load in both armchair and zigzag direction. The modulus and the ultimate stress and also the fracture strain of each single layer and heterostructure under tensile and shear load have been obtained from stress-strain curves. The resulted young modulus and the shear modulus of hBN sheet and graphene single layer have been in good agreement with previous experimental and theoretical results. Therefore, it is assumed that the BG and BGB heterostructures properties, which have been extracted by the same approach as that of the single layers, are reliable. The failure scenario of BG and BGB heterostructure is described in order to give some useful insights into proper application of these systems. In addition, the elastic and shear modulus of heterostructure have been computed with the implimentation of the rule of mixture which has rendered smaller values than moduli that are computed by MD simulation due to the existence of Lennard-jones forces between layers in MD. Thus, the ROM could be performed to roughly predict the young modulus and the shear modulus of hBN and graphene heterostructures.

References

[1] Geim AK, Grigorieva IV. Van der Waals heterostructures. Nature. 2013;499(7459):419.
[2] Wang M, Yan C, Ma L, Hu N, Chen M. Effect of defects on fracture strength of graphene sheets. Computational Materials Science. 2012;54:236–239.
[3] Ni Z, Bu H, Zou M, Yi H, Bi K, Chen Y. Anisotropic mechanical properties of graphene sheets from molecular dynamics. Physica B: Condensed Matter. 2010;405(5):1301–1306.
[4] Zhang Y, Pei Q, Wang C. Mechanical properties of graphynes under tension: a molecular dynamics study. Applied Physics Letters. 2012;101(8):081909.
[5] Novoselov K, Mishchenko A, Carvalho A, Neto AC. 2D materials and van der Waals heterostructures. Science. 2016;353(6298):aac9439.

[6] Dean CR, Young AF, Meric I, Lee C, Wang L, Sorgenfrei S, et al. Boron nitride substrates for high-quality graphene electronics. Nature nanotechnology. 2010;5(10):722.
[7] Woods C, Britnell L, Eckmann A, Ma R, Lu J, Guo H, et al. Commensurate–incommensurate transition in graphene on hexagonal boron nitride. Nature physics. 2014;10(6):451.
[8] Neek-Amal M, Peeters F. Graphene on boron-nitride: Moiré pattern in the van der Waals energy. Applied Physics Letters. 2014;104(4):041909.
[9] Mayorov AS, Gorbachev RV, Morozov SV, Britnell L, Jalil R, Ponomarenko LA, et al. Micrometer-scale ballistic transport in encapsulated graphene at room temperature. Nano letters. 2011;11(6):2396–2399.
[10] Wang H, Taychatanapat T, Hsu A, Watanabe K, Taniguchi T, Jarillo-Herrero P, et al. BN/graphene/BN transistors for RF applications. IEEE Electron Device Letters. 2011;32(9):1209–1211.
[11] Plimpton S. Fast parallel algorithms for short-range molecular dynamics. Journal of computational physics. 1995;117(1):1–19.
[12] Stukowski A. Visualization and analysis of atomistic simulation data with OVITO–the Open Visualization Tool. Modelling and Simulation in Materials Science and Engineering. 2009;18(1):015012.
[13] Stuart SJ, Tutein AB, Harrison JA. A reactive potential for hydrocarbons with intermolecular interactions. The Journal of chemical physics. 2000;112(14):6472–6486.
[14] Dewapriya M, Phani AS, Rajapakse R. Influence of temperature and free edges on the mechanical properties of graphene. Modelling and Simulation in Materials Science and Engineering. 2013;21(6):065017.
[15] Xu L, Wei N, Zheng Y. Mechanical properties of highly defective graphene: from brittle rupture to ductile fracture. Nanotechnology. 2013;24(50):505703.
[16] Lu Q, Gao W, Huang R. Atomistic simulation and continuum modeling of graphene nanoribbons under uniaxial tension. Modelling and Simulation in Materials Science and Engineering. 2011;19(5):054006.
[17] Sevik C, Kinaci A, Haskins JB, Çağın T. Characterization of thermal transport in low-dimensional boron nitride nanostructures. Physical Review B. 2011;84(8):085409.
[18] Jiang JW, Park HS. Mechanical properties of MoS2/graphene heterostructures. Applied Physics Letters. 2014;105(3):033108.
[19] Zhao H, Min K, Aluru N. Size and chirality dependent elastic properties of graphene nanoribbons under uniaxial tension. Nano letters. 2009;9(8):3012–3015.
[20] Zhao H, Aluru N. Temperature and strain-rate dependent fracture strength of graphene. Journal of Applied Physics. 2010;108(6):064321.
[21] Thompson AP, Plimpton SJ, Mattson W. General formulation of pressure and stress tensor for arbitrary many-body interaction potentials under periodic boundary conditions. The Journal of chemical physics. 2009;131(15):154107.
[22] Kumar R, Rajasekaran G, Parashar A. Optimised cut-off function for Tersoff-like potentials for a BN nanosheet: a molecular dynamics study. Nanotechnology. 2016;27(8):085706.
[23] Lee C, Wei X, Kysar JW, Hone J. Measurement of the elastic properties and intrinsic strength of monolayer graphene. science. 2008;321(5887):385–388.
[24] Mahdizadeh SJ, Goharshadi EK, Akhlamadi G. Thermo-mechanical properties of boron nitride nanoribbons: A molecular dynamics simulation study. Journal of Molecular Graphics and Modelling. 2016;68:1–13.

[25] Sakhaee-Pour A. Elastic properties of single-layered graphene sheet. Solid State Communications. 2009;149(1-2):91–95.
[26] Liu X, Metcalf TH, Robinson JT, Houston BH, Scarpa F. Shear modulus of monolayer graphene prepared by chemical vapor deposition. Nano letters. 2012;12(2):1013–1017.
[27] Grimsditch M, Zouboulis E, Polian A. Elastic constants of boron nitride. Journal of applied physics. 1994;76(2):832–834.
[28] Chung JY, Sorkin V, Pei QX, Chiu CH, Zhang YW. Mechanical properties and failure behaviour of graphene/silicene/graphene heterostructures. Journal of Physics D: Applied Physics. 2017;50(34):345302.